Three-dimensional flow measurements in conical and straight wall centrifugal compressor vaneless diffusers

A Pinarbasi, MSc
Department of Mechanical Engineering, University of Cumhuriyet, Sivas, Turkey

M W Johnson, MA, PhD
Department of Mechanical Engineering, University of Liverpool

In the current work three-dimensional flow measurements in two types of centrifugal compressor vaneless diffuser were obtained using hot wire anemometry. The first diffuser was conical, designed to give a constant flow area, while the second straight wall diffuser had a constant axial width. Measurements of mean velocity, flow angle and velocity fluctuation level were obtained on eight cross-sectional planes in each diffuser.

The jet-wake flow pattern and the impeller blade wakes are clearly visible at the inlet of both diffusers. Mixing out of the blade wake proceeds more rapidly in the straight diffuser. The hub boundary layer also develops more rapidly in this diffuser because of the adverse pressure gradient. Velocity fluctuation level measurements highlight the mixing regions within the diffusers.

Recommendations are also made for the design of vaned diffusers. A larger vaneless space would be required with a straight wall diffuser and significant twisting of the vane would be required for both diffuser geometries if significant incidence losses are to be avoided.

Key words: centrifugal compressor vaneless diffuser, hot wire anemometry, conical diffuser, straight wall diffuser

NOTATION

A, B, C	King's law calibration coefficients
E	hot wire anemometer voltage (V)
H, K	directional coefficients for hot wire
L	radial distance from impeller outlet (m)
R_o	impeller outlet radius (m)
u_θ, u_r, u_z	tangential, radial and axial mean velocity components (m/s)
u'_θ, u'_r, u'_z	tangential, radial and axial r.m.s. fluctuating velocity components (m/s)
U_e	effective cooling velocity (m/s)
U_T	peripheral blade velocity (m/s)
y	tangential coordinate in measurement plane (m)
y_o	tangential distance between consecutive blade wakes (m)
z	axial coordinate in measurement plane (m)
z_o	axial diffuser width in measurement plane (m)

1 INTRODUCTION

The overall performance of a centrifugal compressor depends on the good design of the diffuser. The flow is highly non-uniform when it leaves the impeller and the role of the diffuser is to obtain the maximum pressure recovery through mixing out these non-uniformities with minimum loss. The variation in diffuser channel breadth is thus a major design parameter.

Vaneless diffuser flows have been investigated by many researchers [for example Rodgers (**1**), Inoue and Cumpsty (**2**), Senoo *et al.* (**3**) and Clements and Artt (**4**)]. The objective of these studies has generally been to optimize the geometry of the diffuser for maximum pressure recovery. The flow measurements made have revealed some information about the flow structure, but are insufficiently detailed to identify the flow mechanisms responsible for pressure loss.

In the current study (**5**, **6**) a diffuser with a large cross-section is used in order to obtain detailed flow measurements. However, this necessitated the adoption of a low running speed in order to avoid excessive running costs. Thus, the effect of flow compressibility (for example shock waves) could not be investigated but, because the value of the Reynolds number is similar to that for a small high-speed machine, the flow features associated with the mixing out of the flow are typical.

The objective of the current paper is to present results for flow within a conical (constant cross-sectional area) and a straight wall (increasing cross-sectional area) vaneless diffuser.

2 EXPERIMENTAL PROCEDURE

A schematic of the low-speed centrifugal compressor rig used in the study is shown in Fig. 1. The impeller was a De Havilland Ghost impeller, the geometry of which is given by Johnson and Moore (**7**). In the current study, the original radial outlet section was replaced to provide a 30° backswept outlet angle, which is typical of modern machines as described by Pinarbasi and Johnson (**5**). Two types of vaneless diffuser were tested. The first had straight walls and hence a constant axial width, whereas in the second the shroud wall was replaced by a conical wall which resulted in a passage of constant cross-sectional area. The conical diffuser had a shroud face angle of 7°. The diffuser geometries are shown in Fig. 2. Each diffuser discharged directly into the laboratory. The geometry, operating conditions and measurement stations are also summarized in Table 1.

The MS was received on 4 August 1994 and was accepted for publication on 14 July 1995.

C06894 © IMechE 1996

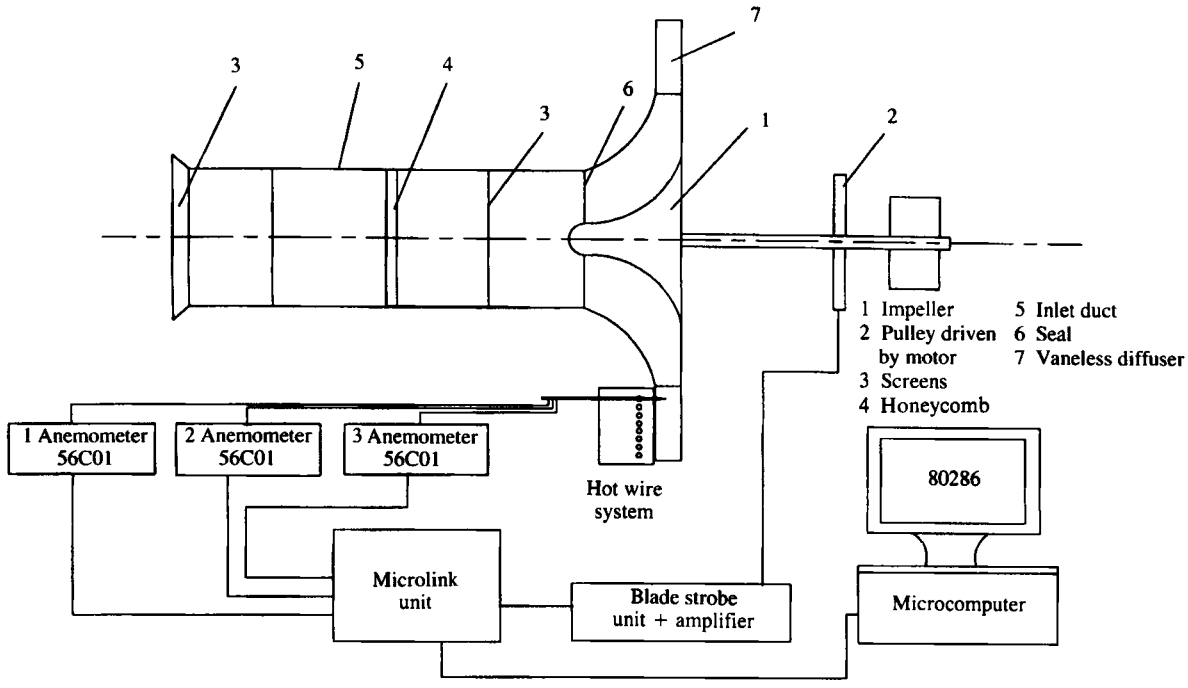


Fig. 1 Schematic test rig

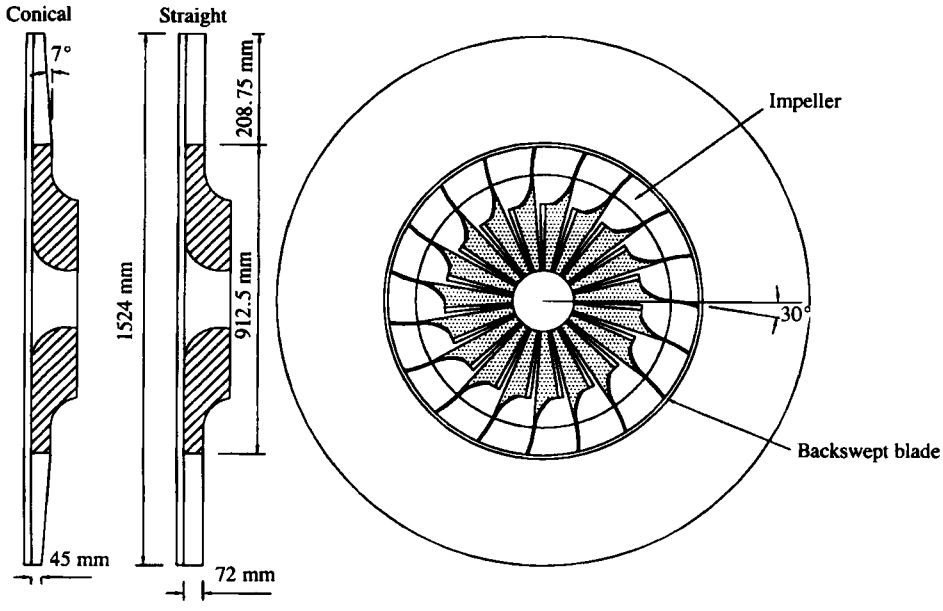


Fig. 2 Diffuser details

Table 1 Geometry, operating condition and measurement locations

Impeller geometry and operating condition	
Inlet blade radius at the hub	$R_h = 88.75$ mm
Inlet blade radius at the shroud	$R_s = 283.75$ mm
Outlet radius	$R_o = 454.6$ mm
Backswept blade angle	$\beta = 30°$
Number of blades	$N = 19$
Conical diffuser cone angle	$\alpha = 7°$
Straight wall diffuser axial width	$b = 72.3$ mm
Mass flowrate	$\dot{m} = 0.142$ kg/s
Rotating speed	$n = 500$ rpm

Measurement locations

Station	1	2	3	4	5	6	7	8
L/R_o	0.02	0.08	0.15	0.21	0.27	0.33	0.39	0.45

© IMechE 1996

2.1 Instrumentation and measurement technique

Triple hot wires were utilized to measure the velocities within the diffuser and were arranged within a measurement volume of size 5 × 5 × 5 mm. A single hot wire probe (Dantec 55P11), aligned circumferentially, was used in combination with a double wire probe (Dantec 55P61), arranged with each wire in the axial–radial plane and at 45° to both the axial and radial directions (see Fig. 3). This mutually perpendicular arrangement of wires was therefore capable of resolving the axial, circumferential and radial velocity components and the directional sign of the axial component. It was assumed that the radial and circumferential components remained positive throughout the flow. There was no evidence in the results of either of these components reducing to zero and hence this assumption was justified.

The hot wires were connected to three constant-temperature hot wire anemometer bridges. The wires were then calibrated in two stages in a wind tunnel, following the procedure of Jørgensen (**8**). In the first stage, the velocity–voltage relationship was established with the wire perpendicular to the flow direction. King's law,

$$E^2 = A + BU_e^c \tag{1}$$

was then fitted to the data for each wire using a least r.m.s. error technique to establish the calibration coefficients A, B and C. The second stage of calibration was achieved by varying the wire orientation at fixed wind tunnel velocity to establish the directional coefficients K and H, where

$$U_e^2 = U_n^2 + KU_t^2 + HU_b^2 \tag{2}$$

U_n, U_t and U_b being the normal, tangential and binormal velocity components relative to the wire. K and H were also obtained by a least r.m.s. error curve-fitting procedure.

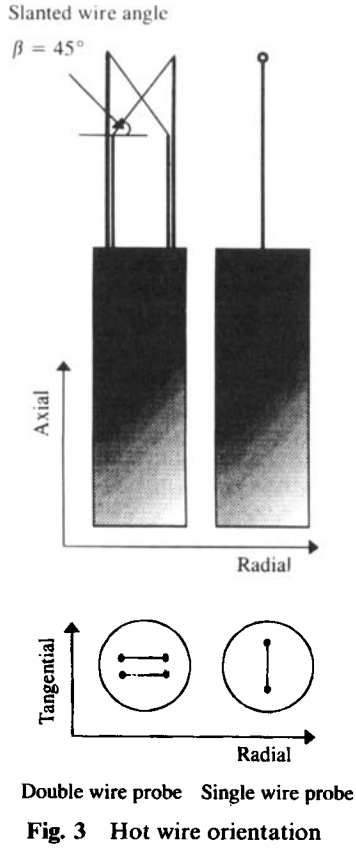


Fig. 3 Hot wire orientation

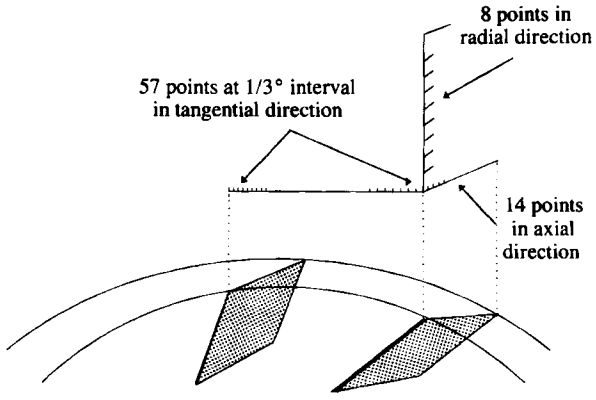


Fig. 4 Measurement point mesh within diffuser passage

An optical shaft encoder provided a pulse for every 1/3° of impeller rotation. This was used to trigger the simultaneous sampling of the three anemometer voltages through a Microlink data acquisition unit. Previous work has shown that the impeller passage-to-passage variations are less than 3 per cent and so in the present study measurements were limited to one of the 19 impeller passages. Readings from 57 circumferential measurement points spanning this impeller passage were logged on each of 230 consecutive impeller revolutions (see Fig. 4). In the straight wall diffuser 14 axial measurement locations were used at 5 mm increments, but this reduced to 10–13 locations within the conical diffuser. Eight radial measurement stations were used in each diffuser.

2.2 Analysis of results

The 230 readings obtained at each measurement point for each of the three anemometers were used to compute the mean velocity components and Reynolds stress tensor using the calibration coefficients. The flowrate was also computed by numerical integration of the radial velocity component over each of the measurement planes, as shown in Table 2. The maximum deviation of this flowrate from the mean for all stations was 4.8 per cent, which gives an indication of the overall experimental accuracy.

3 EXPERIMENTAL RESULTS

3.1 Mean velocity results

At each station the radial velocity is represented by contours and the remaining tangential and axial velocities

Table 2 Flowrates (kg/s) determined through integration of the radial velocity

Station number	Straight diffuser	Conical diffuser
1	0.140	0.137
2	0.138	0.139
3	0.144	0.138
4	0.145	0.144
5	0.142	0.143
6	0.140	0.141
7	0.141	0.145
8	0.143	0.145

© IMechE 1996

by an arrow. The circumferential extremes of each diagram correspond to positions radially in line with the two impeller passage blades.

3.1.1 Station 1

The highly non-uniform flow at station 1 close to the diffuser inlet is shown in Fig. 5. The radial velocity distributions are similar in the two diffusers, but the tangential velocity is generally lower within the straight diffuser. The passage wake is located on the shroud towards the pressure side and the blade wake is clearly visible on the suction side. The secondary flows are, however, much stronger in the conical diffuser where an anticlockwise passage vortex, which is characteristic of backswept impeller discharge flows (**9**, **10**), is apparent. This vortex appears to be suppressed in the straight wall diffuser as a result of the greater slip of the flow relative to the blades at the impeller outlet. These results imply that the downstream geometry of the diffuser has a strong influence on the upstream impeller flow.

3.1.2 Station 2

Between stations 1 and 2 (Fig. 6) the passage and blade wakes are convected in the pressure side to suction side direction by the tangential velocity. The lower tangential velocity in the straight diffuser results in convection over a shorter distance. The blade wake has mixed out significantly at station 2 and is barely discernible in the straight diffuser at $y/y_o = 0.08$. A decrease in the radial velocities due to the increase in flow area (conservation of mass) is also apparent in the straight diffuser, as discussed by Rodgers (**1**).

3.1.3 Station 3

The decrease in radial velocity through the straight diffuser moderates the effect of the lower tangential velocity on the convection of the passage wake. Thus the movement of the passage wake along the shroud is similar between stations 2 and 3 (Fig. 7) in the two diffusers. The blade wake is no longer identifiable in the straight diffuser, but in the conical diffuser it is located at $y/y_o = 0.2$. The blade wake will have taken longer to reach this station in the straight diffuser because of the lower radial velocity, and hence mixing out would be expected to be more advanced. The increase in flow area in the straight diffuser results in an adverse pressure gradient, with associated thickening of the hub wall boundary layer. This also has the effect of displacing the highest velocity region or 'jet' towards the centre of the straight diffuser passage.

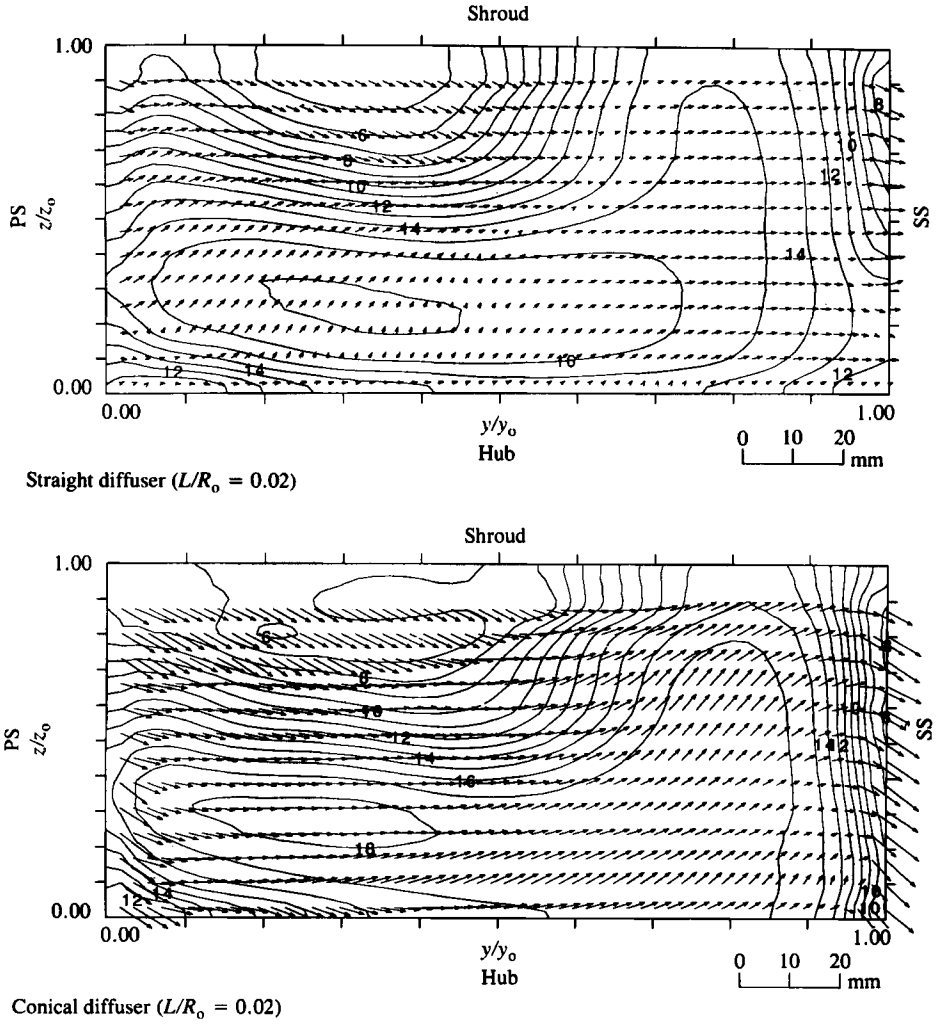


Fig. 5 Mean velocities at station 1 for straight and conical wall diffusers

© IMechE 1996

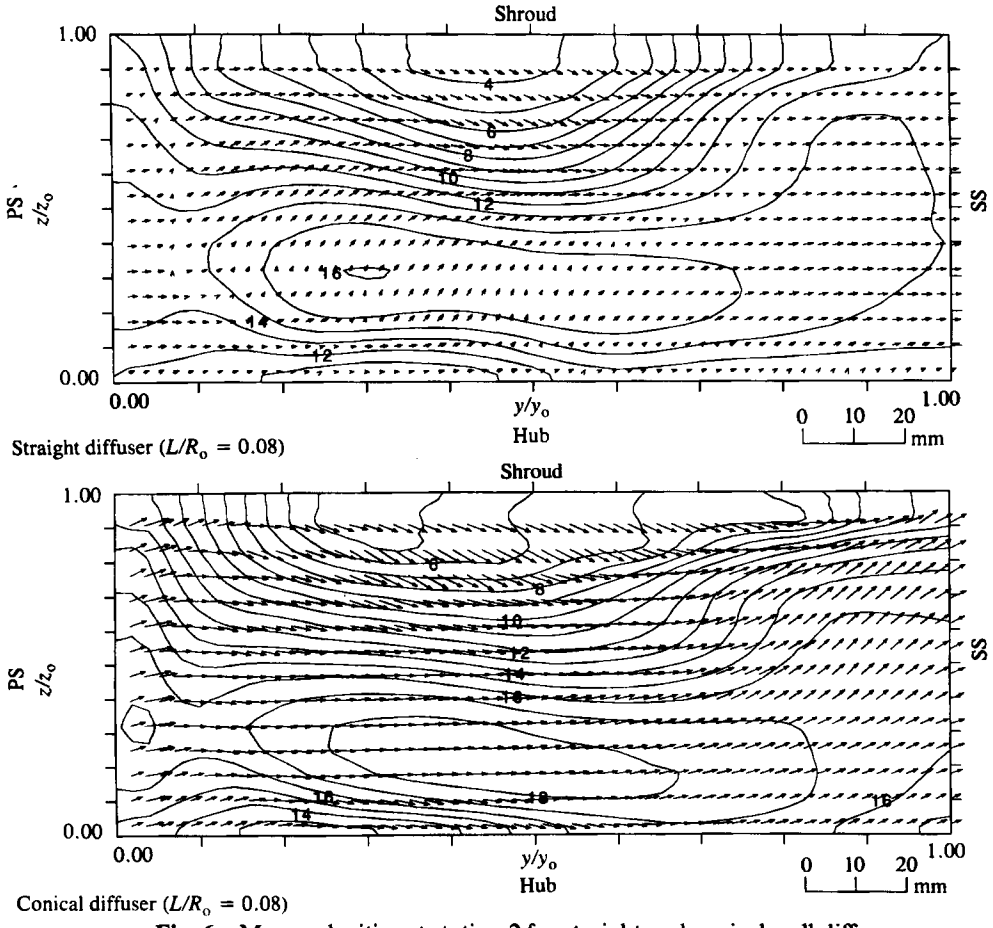


Fig. 6 Mean velocities at station 2 for straight and conical wall diffusers

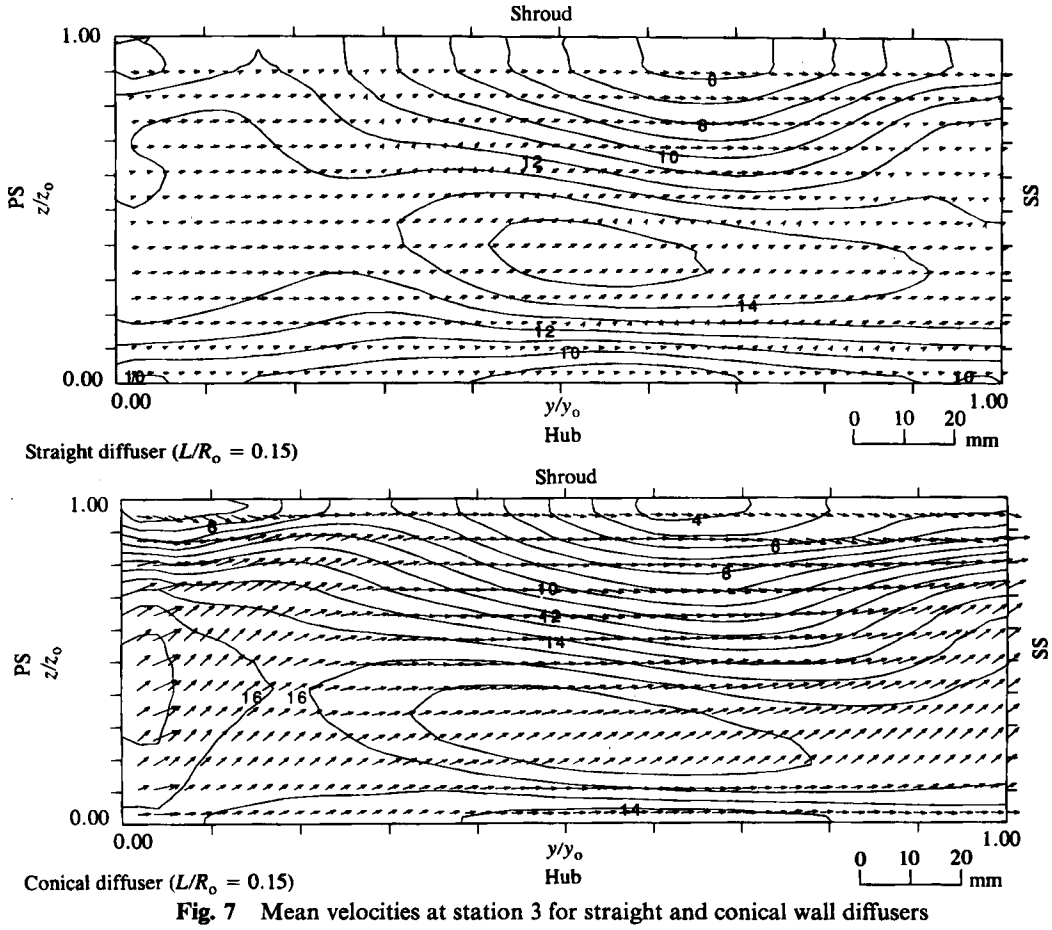


Fig. 7 Mean velocities at station 3 for straight and conical wall diffusers

© IMechE 1996

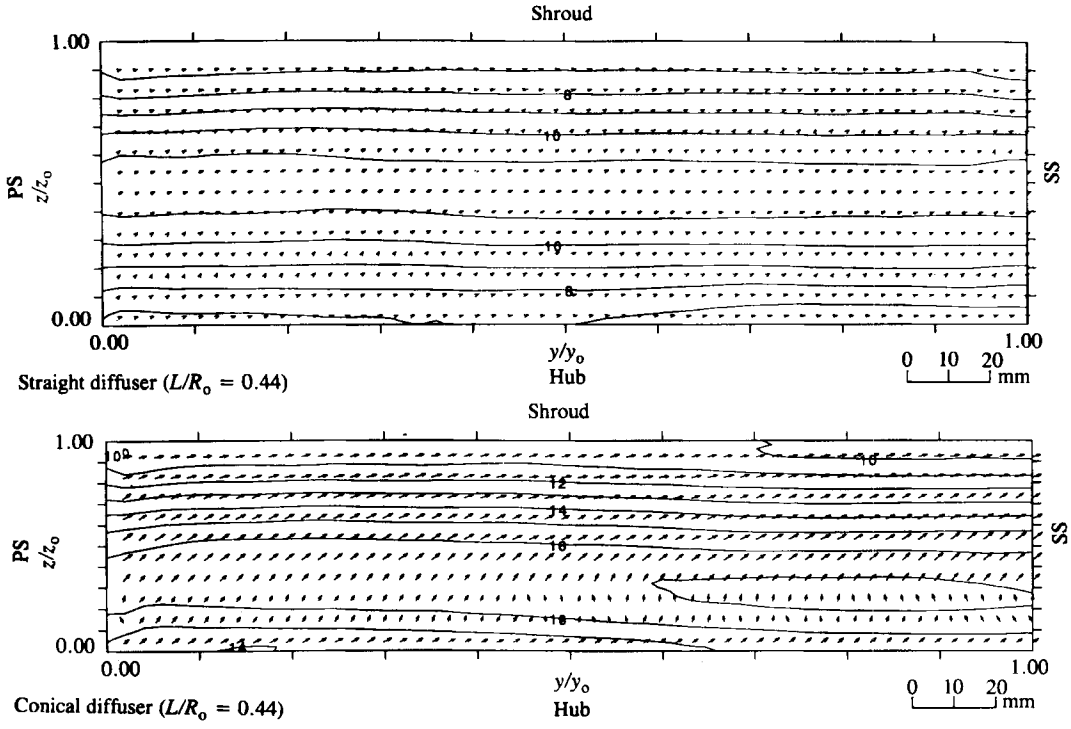


Fig. 8 Mean velocities at station 8 for straight and conical wall diffusers

3.1.4 Station 8

Through stations 4 to 7, flow variations in the circumferential direction are mixed out and a Poiseuille flow (fully developed flow between parallel plates) is gradually established between the two diffuser walls. In the straight diffuser this process is virtually complete at station 8 (Fig. 8), as the flow is virtually symmetric with equal thickness of hub and shroud boundary layers. In the conical diffuser, the hub boundary layer has developed more slowly and hence some asymmetry exists. A significant hub-to-shroud axial velocity results from the blockage caused by the thickening hub boundary layer.

3.2 Flow angle results

3.2.1 Station 1

The lower tangential velocities in the straight diffuser at station 1 result in a lower flow angle, defined by $\tan^{-1}(u_\theta/u_r)$, as shown in Fig. 9. If these flow angles are used to compute the slip factors, it is found that the value for the conical diffuser is almost 1 (zero slip), but the value in the straight diffuser drops to 0.69. This represents a significant change for the impeller and suggests that the impeller is better matched to the conical diffuser than the straight one.

The flow angle can be used in choosing a suitable vaned diffuser blade angle. The variation in flow angle between hub and shroud is up to 40° in the conical and up to 50° in the straight wall diffuser, but this variation can, in principle, be accommodated by twisting the vane leading edge. The variation in the circumferential direction can lead to some incidence losses on the blade. This variation is fairly small (10–20°) near the hub, but is more than 40° near the shroud, where incidence losses would be inevitable. A vaneless space extending beyond station 1 would therefore be recommended for a vaned diffuser. An alternative would be to use a vane that has its leading edge at station 1 near the hub but is swept back to station 2 or 3 near the shroud. For a high-speed compressor, increasing the vaneless space will also increase the diffuser throat area and hence increase the choke limit.

3.2.2 Station 2

At station 2 (Fig. 10), the circumferential variation in flow angle has moderated to about 20° near the shroud in the conical diffuser and hence a vane leading edge at this station may have only small incidence losses. In the case of the straight diffuser, the flow angle variation is still around 40°.

3.2.3 Station 3

In the straight diffuser, the circumferential variation in flow angle near the shroud is reduced to about 25° at station 3 (Fig. 11). A vaneless space near the shroud extending to this station would therefore be recommended for the straight diffuser.

3.3 Velocity perturbation level

The dimensionless velocity perturbation level is defined here as

$$\frac{\sqrt{(u_\theta'^2 + u_r'^2 + u_z'^2)}}{2U} \tag{3}$$

where u_θ', u_r', u_z' are the tangential, radial and axial r.m.s. fluctuating velocity components and $U = (u_\theta^2 + u_r^2 + u_z^2)^{1/2}$ is the mean flow velocity. The velocity fluctuation level is dissipated by viscosity rather than resulting in a pressure recovery. It is therefore useful to identify flow mechanisms that result in the generation of turbulence and hence velocity fluctuations so that the diffuser designer can try to reduce their effect.

© IMechE 1996

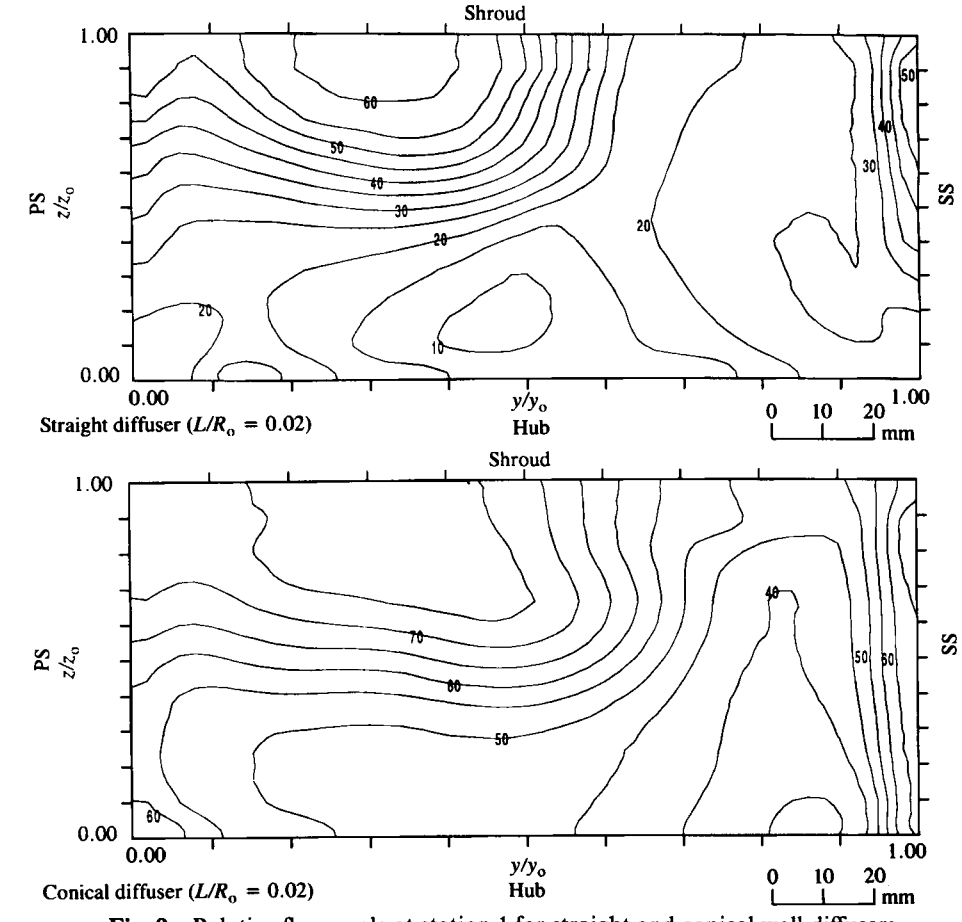


Fig. 9 Relative flow angle at station 1 for straight and conical wall diffusers

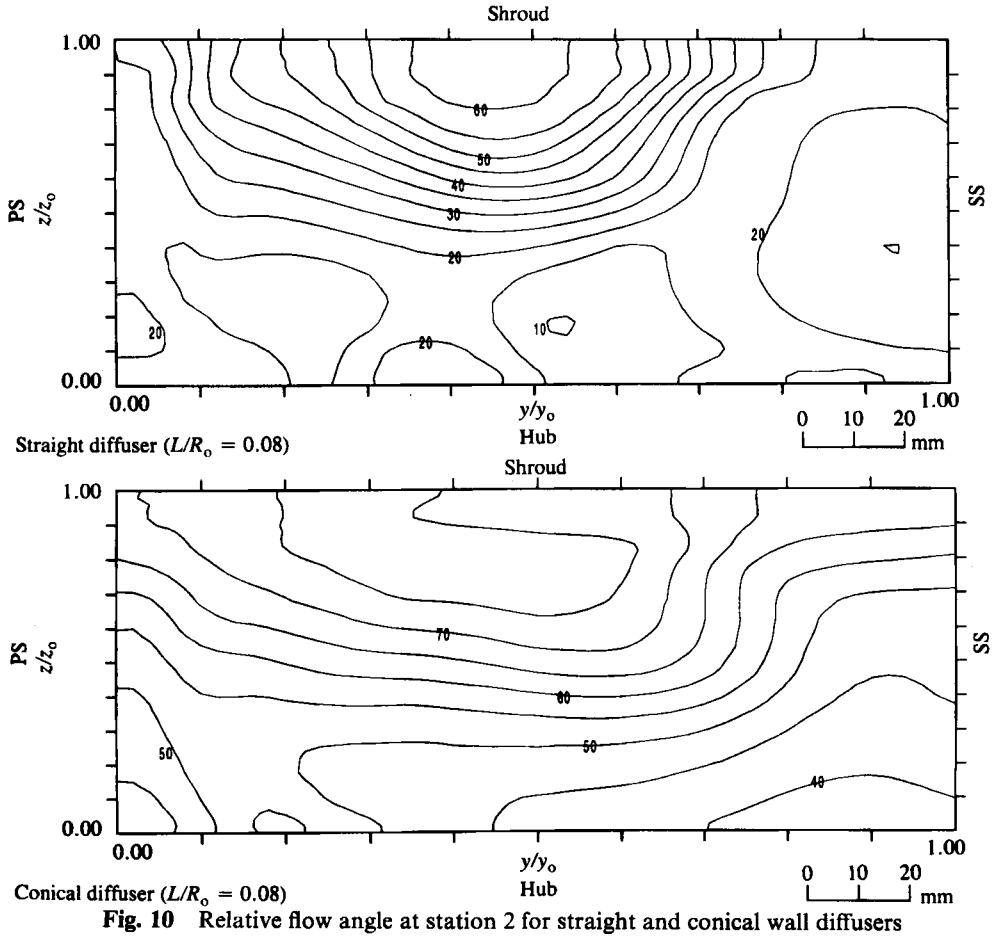
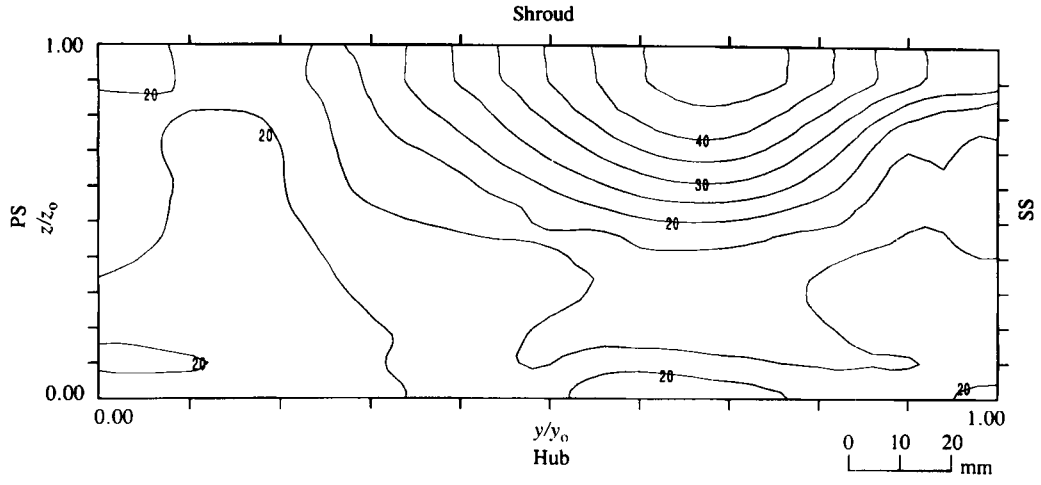
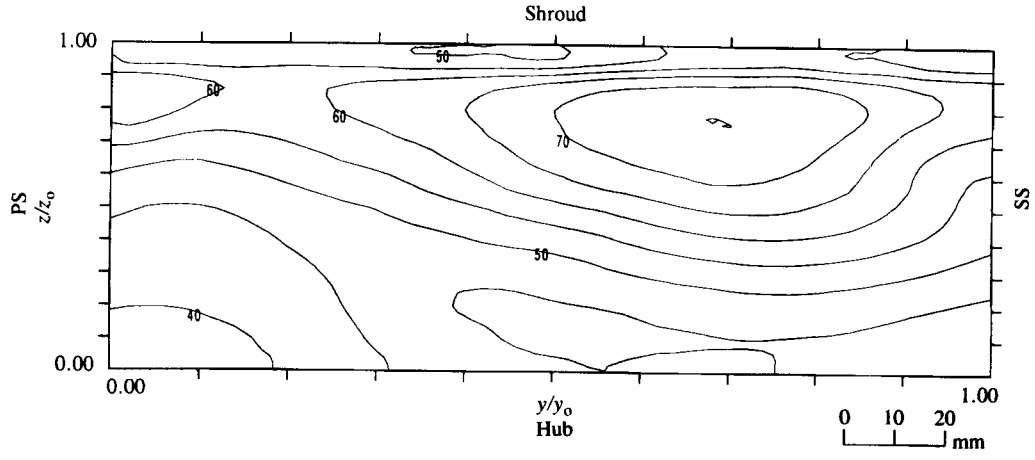


Fig. 10 Relative flow angle at station 2 for straight and conical wall diffusers

© IMechE 1996



Straight diffuser (L/R_o = 0.15)



Conical diffuser (L/R_o = 0.15)

Fig. 11 Relative flow angle at station 3 for straight and conical wall diffusers

3.3.1 Station 1

The pattern of variation in velocity fluctuation is similar in the two diffusers at station 1 (Fig. 12). However, the levels in the conical diffuser are nearly double those in the straight diffuser. This may in part be due to the lower tangential and axial velocities in the straight diffuser which also results in lower fluctuations in these directions. An interesting feature is that the level within the passage wake exceeds that in the blade wake for the straight diffuser whereas the converse is true for the conical diffuser. The fluctuations generated within the passage wake are believed to be due to meandering of the wake position (**5, 11**). It is therefore possible that the adverse pressure gradient increases the instability of the passage wake position. It is also observed that the fluctuation levels in the hub boundary layer are greatly enhanced in the straight diffuser, again due to the adverse pressure gradient and resultant boundary layer thickening.

3.3.2 Station 2

At station 2 (Fig. 13), the levels within the blade wake have decreased substantially as the mixing out of the blade wake is largely complete. The levels within the passage wake have not noticeably decreased from station 1. The velocity fluctuations within the hub boundary layer in the straight diffuser have increased from station 1 as the boundary layer continues to thicken in the adverse pressure gradient.

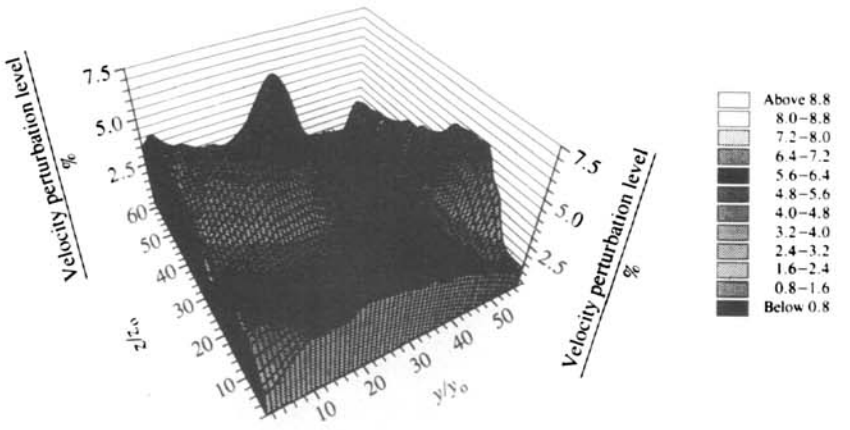
3.3.3 Station 3

At station 3 (Fig. 14), the blade wakes are still discernible, but the levels within the passage wake are now substantially higher. There is now some evidence of mixing within the hub boundary layer in the conical diffuser.

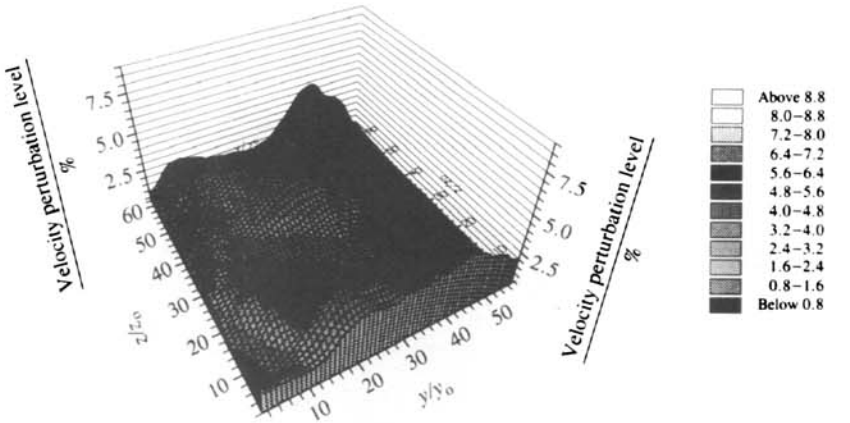
3.3.4 Station 8

The fluctuation levels at station 8 (Fig. 15) complement the mean velocity results (Fig. 8). In the straight diffuser, the levels within the hub and shroud boundary layers are similar, but in the conical diffuser an asymmetric distribution is observed because of the relatively thin hub boundary layer.

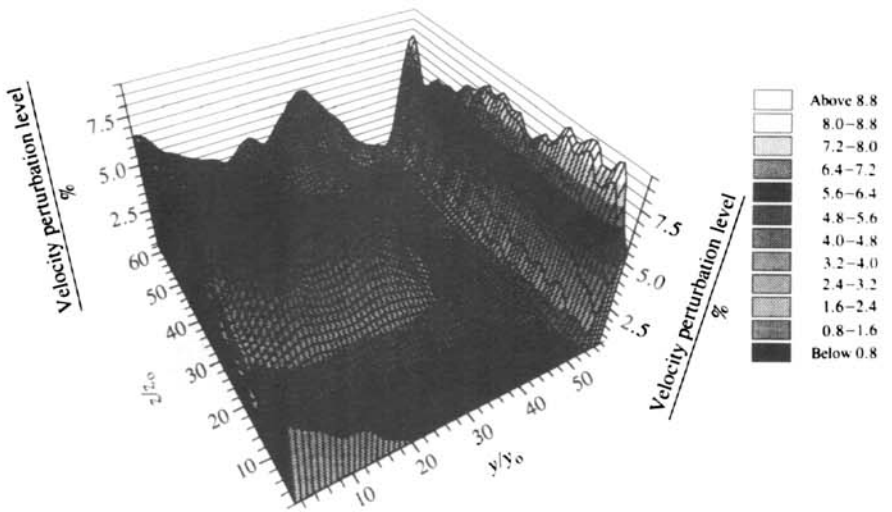
© IMechE 1996



Straight diffuser (L/R_0 = 0.02)

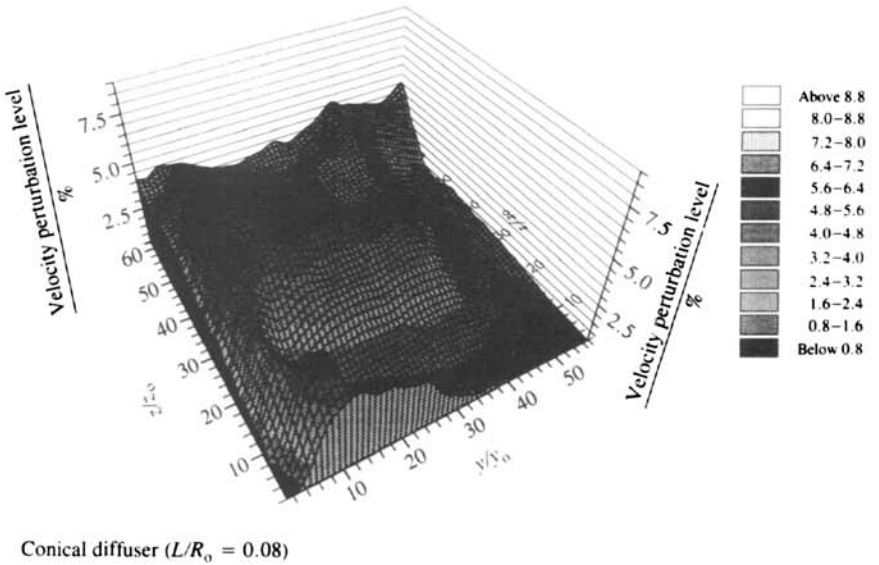


Straight diffuser (L/R_0 = 0.08)



Conical diffuser (L/R_0 = 0.02)

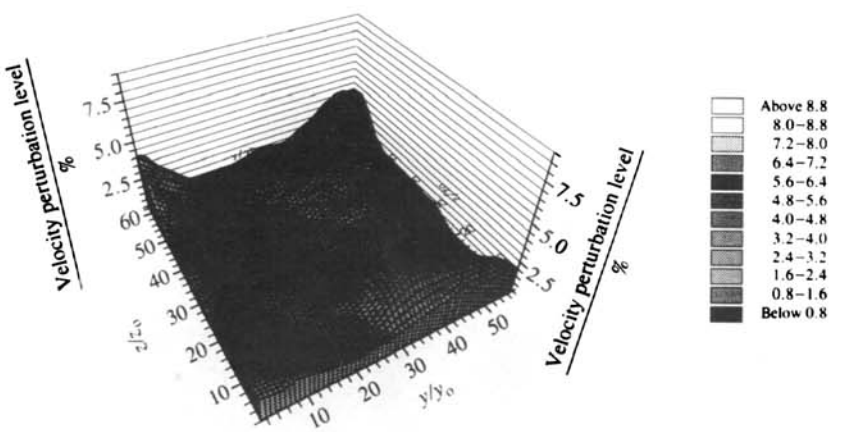
Fig. 12 Velocity perturbation levels at station 1 for straight and conical wall diffusers



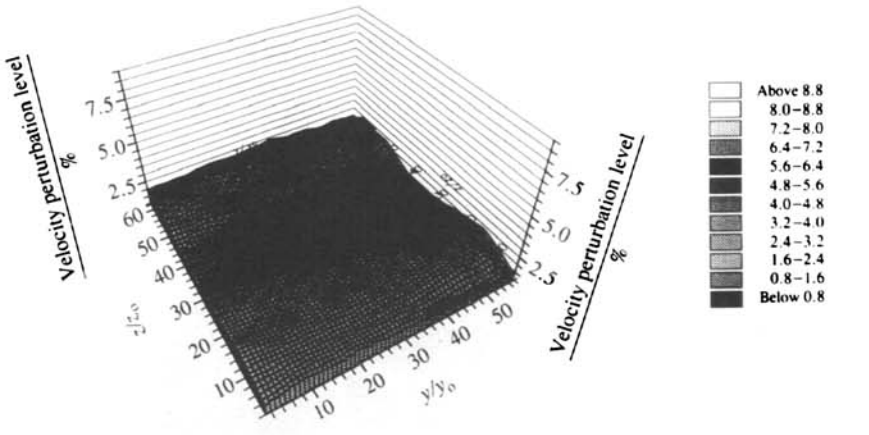
Conical diffuser (L/R_0 = 0.08)

Fig. 13 Velocity perturbation levels at station 2 for straight and conical wall diffusers

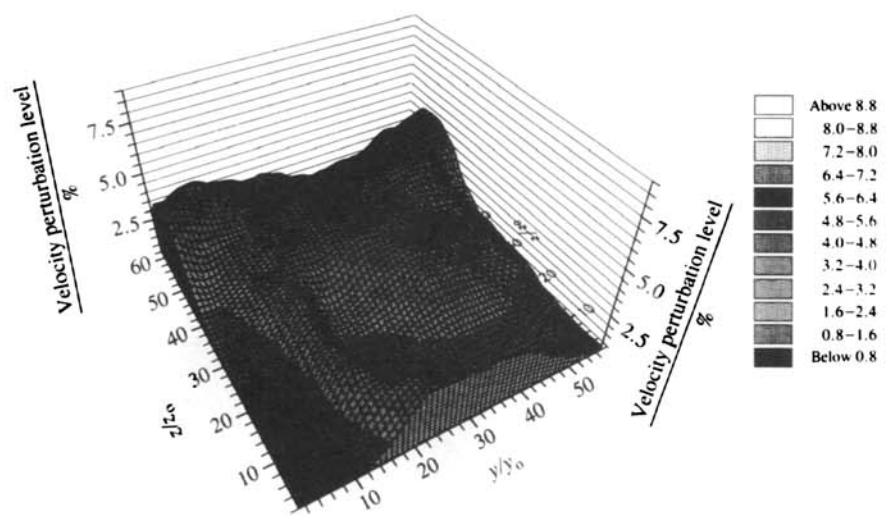
© IMechE 1996



Straight diffuser (L/R_0 = 0.15)

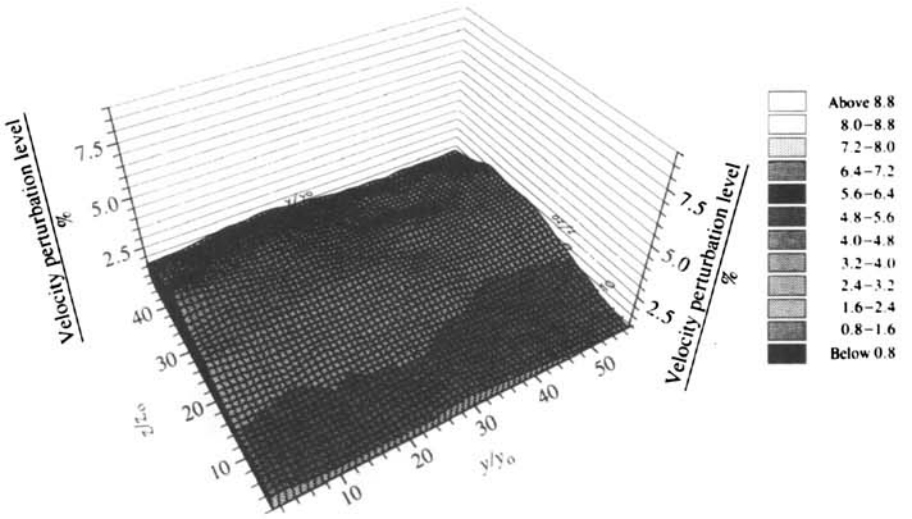


Straight diffuser (L/R_0 = 0.44)



Conical diffuser (L/R_0 = 0.15)

Fig. 14 Velocity perturbation levels at station 3 for straight and conical wall diffusers



Conical diffuser (L/R_0 = 0.44)

Fig. 15 Velocity perturbation levels at station 8 for straight and conical wall diffusers

© IMechE 1996

4 CONCLUSIONS

1. Similar radial velocity distributions were observed at the inlet to both diffusers. The passage and blade wakes were clearly identifiable in similar positions. However, a passage vortex was only observed in the conical diffuser, where less slip resulted at the impeller exit.
2. The lower tangential velocities in the straight diffuser convect the passage and blade wakes in the pressure to suction side direction more slowly in the early part of the diffuser. The increasing flow area in this diffuser tends to moderate this effect beyond station 2.
3. Mixing out of the blade and passage wake proceeds more rapidly in the straight diffuser. This is due, at least in part, to the greater time that the mixing flow spends in the diffuser due to the decreasing radial velocity.
4. Comparison of flow angle results for straight wall and conical diffusers suggests that, for the straight wall design a longer vaneless space and greater twisting of the diffuser vanes would be necessary to avoid significant incidence losses in a vaned diffuser.
5. The velocity fluctuation levels are higher in the conical diffuser. This may be partly due to the higher mean velocities observed in this diffuser. There is also evidence that the meandering of the passage wake location may be greater in the straight diffuser.

REFERENCES

1 **Rodgers, C.** Static pressure recovery characteristics of some radial vaneless diffusers. *Can. Aeronaut. and Space J.*, 1984, **30**(1), 42–54.

2 **Inoue, M.** and **Cumpsty, N. A.** Experimental study of the centrifugal impeller discharge flow in vaneless diffusers. *J. Engng for Gas Turbines and Power*, 1984, **106**, 455–467.

3 **Senoo, Y., Kinoshita, Y.** and **Ishida, M.** Asymmetric flow in vaneless diffusers of centrifugal blowers. *Trans. ASME, J. Fluids Engng*, 1977, **99**, 104–113.

4 **Clements, W. W.** and **Artt, D. W.** The influence of diffuser channel length–width ratio on the efficiency of a centrifugal compressor. *Proc. Instn Mech. Engrs, Part A*, 1988, **202**(A3), 163–169.

5 **Pinarbasi, A.** and **Johnson, M. W.** Detailed flow measurements in a centrifugal compressor vaneless diffuser. *Trans. ASME, J. Turbomachinery*, 1994, **116**(3), 453–461.

6 **Pinarbasi, A.** and **Johnson, M. W.** Detailed stress measurements in a centrifugal compressor vaneless diffuser. *Trans. ASME, J. Turbomachinery*, 1995, **117**, 602–610.

7 **Johnson, M. W.** and **Moore, J.** The development of wake flow in a centrifugal compressor. *Trans. ASME, J. Engng for Power*, 1980, **102**, 383–390.

8 **Jørgensen, F. E.** Directional sensitivity of wire and fibre film probes. DISA information 11, 1971, pp. 31–37.

9 **Krain, H.** Swirling impeller flow. *Trans. ASME, J. Turbomachinery*, 1988, **110**, 122–128.

10 **Fargè, T. Z.** and **Johnson, M. W.** The effect of backswept blading on the flow in a centrifugal compressor impeller. ASME paper 90-GT-231, 1990.

11 **Hathaway, M. D., Chriss, R. M., Wood, J. R.** and **Strazisar, A. J.** Experiment and computation of the NASA low speed centrifugal compressor field. ASME paper 92-GT-213, 1992.

© IMechE 1996